

Forced Boiling of Nanofluids, Effects of Contact Angle and Surface Wettability

Miromid HASHEMINIA¹, Masoud HAGHSHENAS FARD*¹, S. Gholamreza ETEMAD¹, and S. Hasan HASHEMABADI²

* Corresponding author: Tel.: ++98 (311)3915647; Fax: ++98 (311)3912677; Email: haghshenas@cc.iut.ac.ir

1: Department of chemical engineering, Isfahan University of Technology, Isfahan, Iran
2: Department of Chemical Engineering, Iran University of Science and Technology, Tehran, Iran

Abstract Nanofluids are the suspension of ultra fine particles in a conventional base fluid which tremendously changes the heat transfer characteristics of the original fluid. In this paper the boiling characteristics of different nanofluids was studied numerically using a CFD approach. Dispersions of Al₂O₃, SiO₂, and ZrO₂ nanoparticles in water at different concentrations (0.1, 0.01 and 0.001% by volume) have been used. Effects of some noticeable parameters such as nanoparticle concentration and temperature profile on the critical heat flux (CHF) have been investigated. The results of CFD simulation based on two-phase models were compared with experimental data. Boiling curves and critical heat flux were measured for the base fluid and the nanofluids. Based on the simulation results, it was concluded that the using of the Zirconium oxide (0.001%) led to modest (up to 31%) increase in the CHF. The minimum enhancement belongs to the aluminum oxide (0.1%) which increases the critical heat flux up to 11%. According to the experimental results, despite of expectation, addition of the nanoparticles causes decreasing the boiling heat transfer coefficient. This reduction is related to the changing of the surface characteristic causing by depositing the nanoparticles. In the Al₂O₃/water and SiO₂/water nanofluids, the surface contact angle increases with increase in the nanoparticle volume fraction, so the CHF decreases.

Keywords: Boiling, Nanofluids, Critical heat flux, Contact angle, CFD

1. Introduction

When liquid coolant undergoes a change in phase due to the absorption of heat from a heated solid surface, a higher transfer rate occurs. Therefore, boiling heat transfer has played an important role in industrial heat transfer processes such as macroscopic heat transfer exchangers in nuclear and fossil power plants, and in microscopic heat transfer devices such as heat pipes and microchannels for cooling electronic chips. The use of boiling is limited by a condition called critical heat flux (CHF), which is also called a boiling crisis or departure from nucleate boiling (DNB) [1-2]. Critical heat flux describes the thermal limit of a phenomenon where a phase change occurs during heating (such as bubbles forming on a metal surface used to heat water), which suddenly decreases the efficiency of heat transfer, thus causing localised overheating of the heating surface. At this point, the bubbles are large enough to merge and form a continuous vapor film between the

liquid phase and the heated surface. Due to lower thermal conductivity of the vapor compared to the liquid, the thermal resistance increases sharply due to the presence of the vapor film, leading to a large increase in wall superheat from about 20 K to about 1000 K. Therefore, The understanding of CHF phenomenon and an accurate prediction of the CHF condition are important for safe and economic design of many heat transfer units including nuclear reactors, fossil fuel boilers, fusion reactors, electronic chips, etc. Mixture of nano-size particles suspended in a base fluid is named nanofluid. The nanofluid has a higher thermal conductivity in comparison with the base fluid. This higher thermal conductivity enhances the rate of heat transfer in industrial applications. Nanofluids are a class of heat transfer fluids created by dispersing solid nanoparticles in traditional heat transfer fluids. Research results show that nanofluids have thermal properties that are very different from those of conventional heat

transfer fluids such as water or ethylene glycol [3]. Recently, the nanofluid was gotten spotlight due to the enormous change in CHF and it was also clarified that increase or decrease in of CHF is come from the change of surface morphology due to the nanoparticle deposition on heater surface. Many experimental and numerical works have been attempted in the nanofluids area [4-14]. Some of these works are focused on the effect of nanofluids on the boiling phenomenon. Some of them show that nanoparticles can change the characteristics of the heating surface and increase the critical heat flux dramatically. CHF enhancement in nanofluids has been widely observed by almost all researchers in convective boiling and in pool boiling. Das et al. presented an experimental study which evaluated the boiling heat transfer of Al_2O_3 nanoparticles suspended in deionized water [4]. The various concentrations of nanoparticles (1 to 4%) were tested. The results showed that the use of nanofluids affected a pronounced increase in the critical heat flux. You et al. reported experimental results which illustrated the Al_2O_3 /Water nanofluids showed CHF enhancement up to 200% [5]. They measured the CHF in pool boiling using a flat, square copper heater submerged with nanofluids at a sub-atmospheric pressure of 2.89psia. Experimental studies of Boiling heat transfer performance and phenomena of Al_2O_3 /water nanofluid from a plain surface in a pool is reported by Beng and Chang [6]. The results showed that in the nanofluid, a 20% decrease in heat transfer rate and a 32% increase in CHF is observed.

Wen and Ding presented an experimental study which evaluated the pool boiling heat transfer of aqueous based gamma-alumina nanofluids [7]. The various concentrations of nanoparticles were tested. The results showed that at concentration of 1.25 wt%, the boiling heat transfer coefficient of the nanofluids was 40% higher than the base fluid.

Ahn et al. [8] investigated aqueous nanofluids with a 0.01% concentration of alumina nanoparticles; CHF was distinctly enhanced under forced convective flow conditions

compared to that in pure water.

Another investigation by Kim et al. [9] also resulted in a similar nanoparticle deposition on the heater surface after nanofluid boiling. They investigated the subcooled flow boiling using dilute alumina, zinc oxide and diamond water-based nanofluids. They measured both the CHF and the heat transfer coefficient during their flow boiling experiments. CHF enhancement was found to increase with both mass flux and nanoparticle concentration for all nanoparticle materials; an increase as great as 53% was observed for CHF.

Dominguez-Ontiveros et al. investigated Al_2O_3 nanoparticles in water, and visually observed their effect on nucleate boiling [10]. They noted a change in the hydrodynamic behavior of bubbles with the addition of nanoparticles to the pure water.

Another experiment that confirms the increasing critical heat flux of nanofluids was investigated by Vassallo et al. [11] who observed the boiling characteristic of silica-water nanofluids with 0.5% volume concentration.

Zhou [12] experimentally investigated the effects of acoustical parameters, nanofluid concentration and fluid subcooling on boiling heat transfer characteristics of a copper-acetone nanofluid. The results showed that the presence of the copper nanoparticles did not affect the dependence of the heat transfer on the acoustic cavities and fluid subcooling. Without an acoustic field, the boiling heat transfer of the nanofluid was reduced.

In the C. Gerardi et al.'s study, Infrared thermometry was used to obtain first-of-a-kind, time- and space-resolved data for pool boiling phenomena in water-based nanofluids at low [13]. The nanoparticles caused deterioration in the nucleate boiling heat transfer (BHT) (by as much as 50%) and an increase in the CHF (by as much as 100%). It was found that a porous layer of nanoparticles built up on the heater surface during nucleate boiling, which improved surface wettability compared with the water-boiled surfaces.

In the present work Computational Fluid Dynamics (CFD) simulation is developed for investigation of forced boiling of nanofluids in

a vertical pipe. Effects of nanoparticles types, nanofluid concentration, and wall heat flux on subcooled boiling have been investigated. The CFD predictions are compared to the experimental results reported by G. G. Bartolomei, and V. M. Chanturiya [14].

2. CFD Simulation:

A two-phase two-fluid CFD model is presented to investigation of the turbulent subcooled flow boiling in a heated vertical pipe. The grid uses the unstructured elements and the number is 8700. Grid independency is also checked in CFD modeling. When the elements number increase, it can induce a very small physical discretization error, which causes the numerical solution approximate to the exact solution. The CFD calculations were performed with Fluent and the geometric modeling and meshing was done using the meshing software, GAMBIT. The schematic domain and operating conditions are shown in figure 1

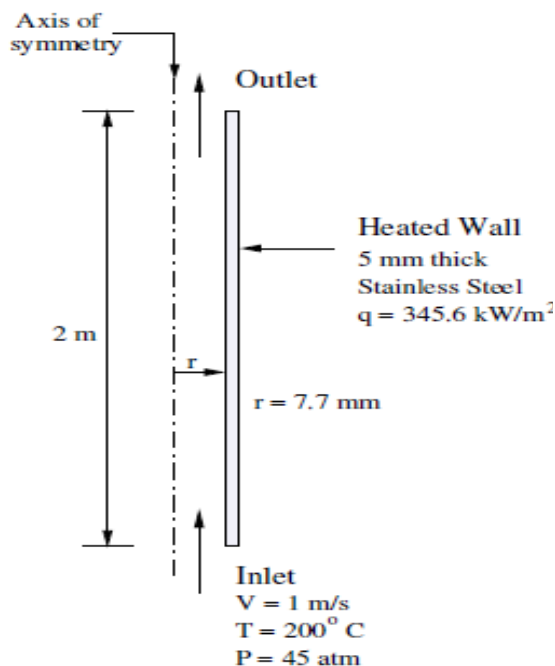


Fig. 1. Schematic of computational domain

At the domain inlet, “velocity inlet” boundary condition was used. The magnitude of the inlet velocity is specified and the direction is taken to be normal to the boundary. At this boundary, the appropriate values for the velocity components and inlet temperature must be specified. At the tube outlet, “outlet

flow” boundary condition was used. At the outlet section flow field is assumed fully developed and relative static pressure is specified over the outlet boundary. No-slip boundary condition with constant wall heat flux was applied at the walls.

Though boiling phenomena is complicated, the thermal convection and diffusion are still governed by the equations of continuity, motion (Navier–Stokes equations) and the equation of energy conservation. So the governing equations are:

Continuity:

$$\frac{\partial \rho}{\partial t} + \nabla \cdot (\rho \mathbf{V}) = 0$$

Momentum:

$$\rho \frac{\partial}{\partial t}(\mathbf{V}) + \nabla \cdot (\mathbf{V}\mathbf{V}) = -\nabla P + \nabla \cdot \boldsymbol{\tau} + S_M$$

$$S_M = (S_{Mx}, S_{My}, S_{Mz})$$

Energy:

$$\rho \frac{DE}{Dt} = -\nabla \cdot (P\mathbf{V}) + \nabla \cdot (\boldsymbol{\tau} \cdot \mathbf{V}) + \nabla \cdot (k\nabla T) + S_E$$

In the present study, two-equation turbulence model, $k - \varepsilon$ model, was used. For the most engineering problems, the $k - \varepsilon$ model has been used with significant success. This model uses an eddy viscosity hypothesis for the turbulence. Alternatively the bubble-induced turbulence may be taken into account directly as additional terms in turbulent transport equations.

In the boiling flow, heat and mass exchange between the phases takes place on the heated wall and in the liquid. The evaporation mass flow on the wall is the total mass of bubbles periodically departing from nucleation sites:

$$\dot{m}_w = \left(\frac{\pi \cdot d_{bw}^3}{6} \right) \rho_g f \cdot N_a,$$

Which:

$$f = \sqrt{\frac{4 \cdot g \cdot (\rho_l - \rho_v)}{3 \cdot d_{bw} \cdot \rho_l}}$$

d_{bw} is the bubble departure diameter, f is the bubble departure frequency and N_a is the nucleation site density. The bubble departure diameter can be calculated using Kostanchuk and Tolubinski model [15]:

$$d_{bw} = 2.42 \times 10^{-5} P^{0.709} \frac{a}{\sqrt{b\Phi}}$$

In this work a modified model of Kurul and Podowski is implemented which splits the total wall heat flux into three different modes of heat transfer [16]:

$$Q_w = Q_c + Q_q + Q_e$$

Where Q_c is the convection heat flux transferred to the liquid phase near the wall, Q_q is quenching heat flux transferred to the subcooled liquid from the bulk and Q_e is the fraction of the wall heat flux, that is directly used to generate vapor bubbles.

$$Q_c = A_{bub} h_c (T_w - T_l)$$

$$Q_e = m^\circ (h_{g,sat} - h_l)$$

$$Q_q = A_{bub} h_q (T_w - T_l)$$

A_{bub} is determined as the bubble influence area per unit wall area:

$$A_{bub} = \min \left[1, N_a K \left(\frac{\pi d_{bw}^2}{4} \right) \right]$$

The parameter K determines the size of the bubble influence area around the nucleation site on the heated wall that is subject to the quenching heat transfer. In order to solve above-mentioned equations the thermo-physical parameters of nanofluids such as density, viscosity, heat capacity, and thermal conductivity must be evaluated. These parameters are defined as follow:

$$\mu_{nf} = (306\phi_{nf}^2 - 0.19\phi_{nf} + 1)\mu_{bf}$$

$$\rho_{nf} = \phi_{nf}\rho_s + (1 - \phi_{nf})\rho_f$$

$$C_{P_{NF}} = \frac{\phi_{nf}\rho_s C_{P_s} + (1 - \phi_{nf})\rho_f C_{P_f}}{\rho_{nf}}$$

$$k_{nf} = (28.905\phi_{nf}^2 + 2.8273\phi_{nf} + 1)k_{bf}$$

Which ϕ_{nf} is the nanofluid volume fraction.

These relations have been used for Al_2O_3 /Water nanofluid by Maiga et al. [17]. For calculation of thermal conductivity in SiO_2 /Water and ZrO_2 /Water nanofluids, Hamilton-crosser's model has been used [18]:

$$\frac{k_{eff}}{k_l} = \frac{k_p + (n-1)k_l - (n-1)(k_l - k_p)\phi}{k_p + (n-1)k_l + (k_l - k_p)\phi}$$

3- Results and discussions:

In order to establish accuracy of the numerical model, the predicted data for different nanofluids (SiO_2/H_2O , ZrO_2/H_2O , and Al_2O_3/H_2O) has been compared to the experimental data reported by G. G. Bartolomei, and V. M. Chanturiya [14]. Subcooled flow boiling in their work was considered in a vertical heated pipe. Subcooled water enters the pipe from the bottom. Uniform heat flux boundary conditions are applied along the pipe wall. A 24 mm diameter pipe with 2m of length is considered. First, the CFD simulation was applied to predict the void fraction ϕ (vapor volume fraction) for subcooled flow boiling of water in a vertical pipe for different heat flux conditions.

The estimated axial void fraction and temperature distribution along the pipe is given in the figure 2.

The numerical results of this study are compared with the experimental data of Bertolemei and Chanturiya [14]. It is seen that the results gotten by CFD in this work and the experimental data are in good agreement.

It is clear that the boiling starts form $X=0.6m$. The vapor volume fraction at the outlet pipe is 62%. For prediction of CHF, the vapor volume fraction should be calculated at various heat fluxes. The CHF is located at the point where the outlet volume fraction is 80%. Figure 3 shows the vapor volume fraction versus the wall heat flux. From this figure it can be found that the CHF of water is about $440KW/m^2$.

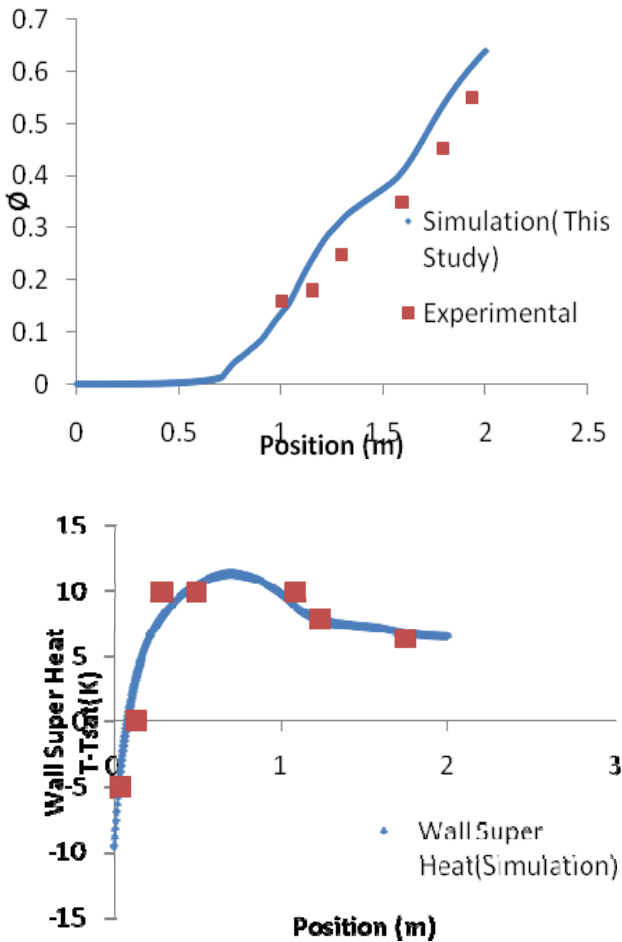


Fig. 2. Axial void fraction and temperature distribution along the pipe

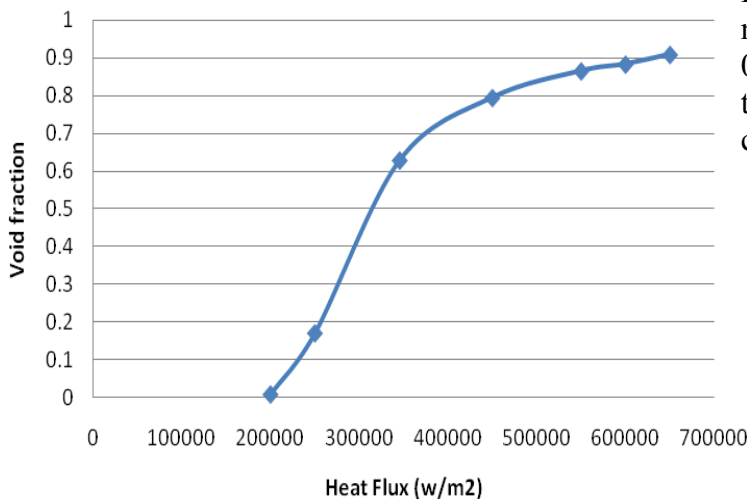


Fig. 3. Vapour volume fraction versus wall heat flux in a vertical pipe

Now we can analyze the boiling of various nanofluids in a vertical pipe. CFD simulation of water-based nanofluids containing Al_2O_3 , ZrO_2 and SiO_2 nanoparticles were conducted. Research on surface characteristics indicates that deposition of nanoparticles on the heating surface is one of the main causes behind the CHF enhancement. Surface wettability, liquid spreadability and morphology are some of the heater surface properties altered by the nanoparticle deposition. Table 1 shows the contact angle of various nanofluids on the different surfaces. It is clear from this table that in the small concentrations, the contact angle of Al_2O_3 and SiO_2 nanofluids is lower than other nanofluids (wettability is higher), and the contact angle increases with decrease in nanofluid concentration. The wettability of the ZrO_2 nanofluid is small in the low concentrations. Effect of Al_2O_3 /water nanofluid concentration on volume fraction at various heat fluxes is shown in Figure 4. It can be seen that the curves shift to the right, so the CHF increases. The CHF in 0.001%v Al_2O_3 nanofluid is 25% higher than water. The CHF decreases by increasing the nanofluid volume fraction. As shown in figure 5 and figure 6, this trend is same for SiO_2 and ZrO_2 nanofluids. But, the contact angle in the 0.001 % (v) ZrO_2 nanofluid is 43° and in the concentration of 0.01 % (v) is 26° . So the increase in CHF in the concentration of 0.01% is higher than other concentrations.

Table 1. Contact angles of various nanofluids

Fluid	Pure water	Al ₂ O ₃			ZrO ₂			SiO ₂		
Concentration	0	0.001	0.01	0.1	0.001	0.01	0.1	0.001	0.01	0.1
Clean surface	79°	80°	73°	71°	80°	80°	79°	71°	80°	75°
Nanofluid boiled surface	8°-36°	14°	23°	40°	43°	26°	30°	11°	15°	21°

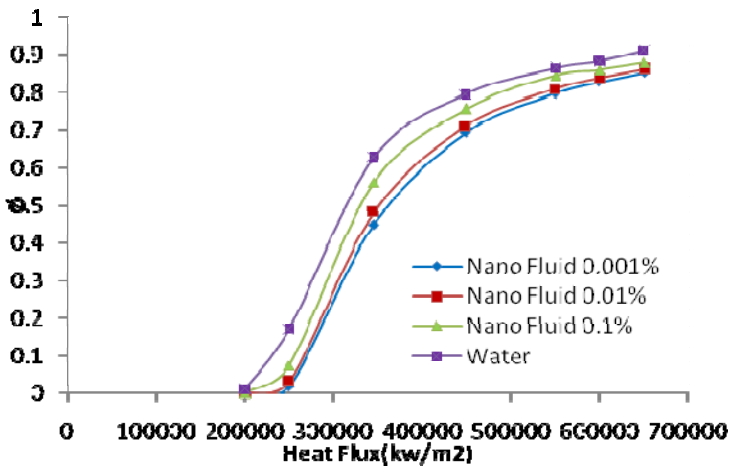


Fig. 4. Effect of Al₂O₃/water nanofluid concentration on vapor volume fraction

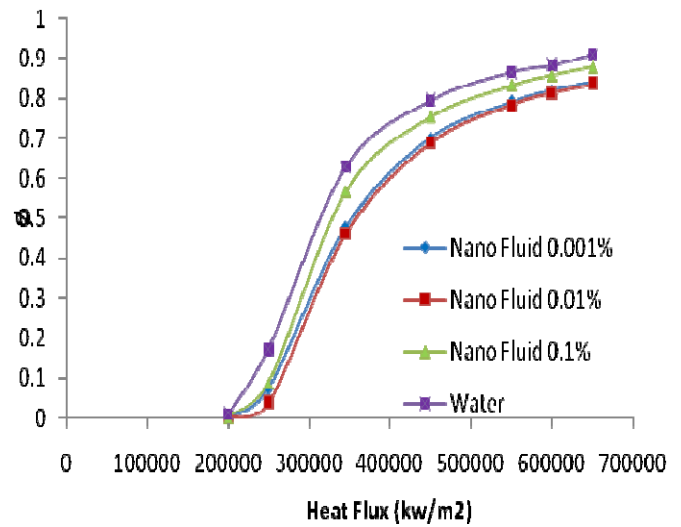


Fig. 6. Effect of ZrO₂/water nanofluid concentration on vapor volume fraction

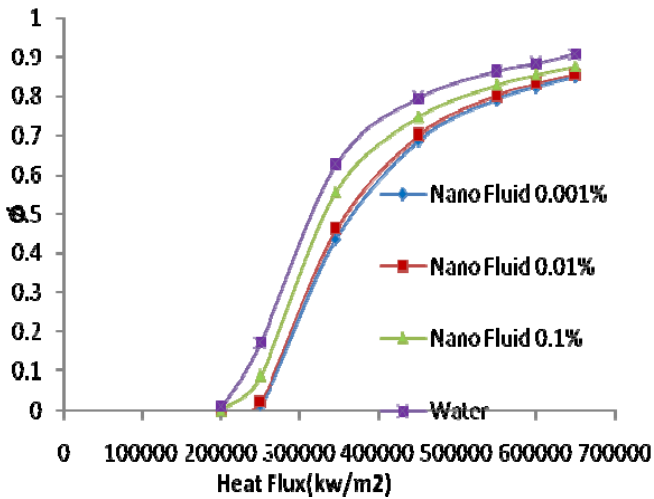


Fig. 5. Effect of SiO₂/water nanofluid concentration on vapor volume

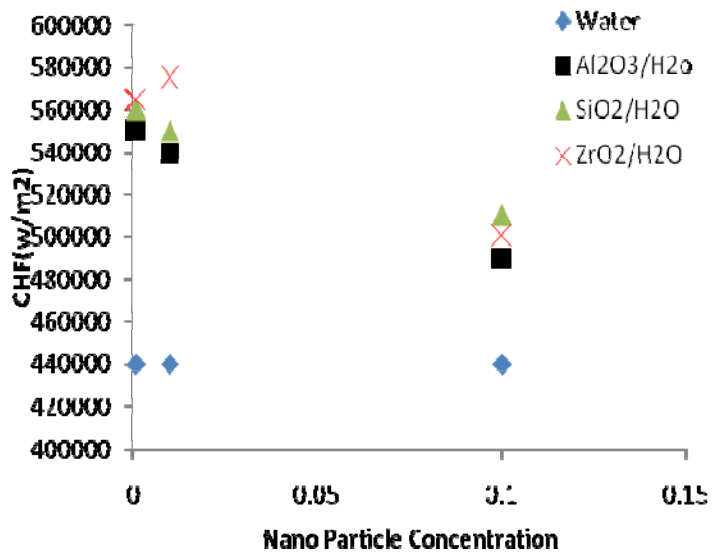


Fig. 7. Effect of various nanofluids on the CHF predicted by CFD

The CHF in three different types of nanofluids in various concentrations is shown in figure 7. As shown in figure 7, The CHF of the base fluid (water) is lower than the nanofluids. Also it is clear that the CHF in Al_2O_3 /water and SiO_2 /water nanofluids decreases with increase in the nanoparticle volume fraction. This trend is reasonable, because the contact angle increases with increase in concentration. That means the number of nucleation sites and the heat transfer coefficient increases. In the ZrO_2 /water nanofluid, the CHF first increases with increase in concentration and then decreases. This procedure is also reasonable because as shown in table 1, the change in contact angle is not same to the other nanofluids. In this case, at the concentration of 0.01%, the number of nucleation sites is lower than other cases, so the CHF increases.

4. Conclusions and Future Works:

This study is focused on the numerical study of subcooled boiling in a vertical pipe under high-pressure conditions using the Computational Fluid Dynamics (CFD). The validation of the results has been made with comparing the CFD predictions with the experimental data in the literature with the same conditions of experience. Grid independent solution on dense grids was obtained by using adequate near-wall treatment. First, the CFD simulation was applied to predict the vapor volume fraction and temperature distribution for subcooled boiling of water in a vertical pipe for different heat flux conditions. The calculated averaged void fraction distributions show reasonable agreement with the experimental data. Then CFD was applied to prediction of the CHF in the various nanofluids. The vapor volume fraction at the outlet pipe has been evaluated for Al_2O_3 /water, ZrO_2 /water and SiO_2 /water nanofluids. The CHF of the base fluid (water) is lower than the nanofluids. Also it can be found from the CFD predictions that the CHF in Al_2O_3 /water and SiO_2 /water nanofluids decreases with increase in the nanoparticle volume fraction. This trend is reasonable, because the contact angle increases with

increase in concentration. This procedure in ZrO_2 /water nanofluid is not same because the change in the contact angle is not same to the other nanofluids. In this nanofluid, the CHF first increases with increase in concentration and then decreases. In this case, at the concentration of 0.01%, the number of nucleation sites is lower than other cases, so the CHF increases. Based on the CFD simulations, the maximum enhancement in CHF is 31% which belongs to the ZrO_2 /water nanofluid with 0.01% of concentration and the minimum enhancement in CHF belongs to Al_2O_3 /water nanofluid which increase the critical heat flux up to 11%. In general, CFD predictions demonstrate that the CFD tool is able to capture the essential physics underlying subcooled boiling of nanofluids and its prediction agrees pretty well with the experimental data.

This is an initial study of the problem and future work will involve consideration of a more comprehensive model incorporating the possible influence on CHF of variables other than the void fraction. An example is the effect of concentration of nano particles on nucleation site densities. In the context of the CFD work it is really desirable to increase the grid density for this geometry. Thereby this will both demonstrate explicit grid convergence and facilitate a comprehensive uncertainty analysis of the data.

5. References:

- [1] Deghal A. L., Chaker, A., 2010, Numerical Study of Subcooled Boiling In Vertical Tubes Using Relap5/Mod3.2, *Journal of Electron Devices* 7, 240-245.
- [2] Meamer E. N., Groeneveld D.C., Cheng, S. C., 2011, Experimental study of inverted annular film boiling in a vertical tube cooled by R-134a, *International Journal of Multiphase Flow* 37, 67-75.
- [3] Barber, J., Brutin, D., and Tadrist, L., 2011, A review on boiling heat transfer enhancement with nanofluids, *Nanoscale Research Letters* 6:280-296.
- [4] Das, S. K., Putra, N., and Roetzel, W., 2003, Pool boiling characteristics of

nano-fluids. *International Journal of Heat and Mass Transfer*, 46(5): 851-862.

[5] You, S. M., Kim, J. H., and Kim, K.H., 2003, Effect of nanoparticles on critical heat flux of water in pool boiling heat transfer. *Applied Physics Letters*, 83(16): 3374-3376.

[6] Bang, I. C. and Chang, S. H., 2005, Boiling heat transfer performance and phenomena of Al₂O₃-water nano-fluids from a plain surface in a pool. *International Journal of Heat and Mass Transfer*, 48(12): 2407-2419.

[7] Wen, D. S. and Ding, Y. L., 2005, Experimental investigation into the pool boiling heat transfer of aqueous based gamma-alumina nanofluids. *Journal of Nanoparticle Research*, 7(2): 265-274.

[8] Ahn, H. S, Kim, H., Jo, Kang S., Chang W., Kim, M. H., 2010, Experimental study of critical heat flux enhancement during forced convective flow boiling of nanofluid on a short heated surface. *Int. J. Multiphase Flow*, 36(5):375-384.

[9] Kim, S. J., et al., 2007, Surface wettability change during pool boiling of nanofluids and its effect on critical heat flux. *International Journal of Heat and Mass Transfer*, (19-20)50 :p. 4105-4116.

[10] Dominguez-Ontiveros E, Fortenberry S, Hassan Y. A, 2010, Experimental observations of flow modifications in nanofluid boiling utilizing particle image velocimetry, *Nuclear Eng Des*, 240(2):299-304.

[11] Vassallo, P., Kumar, R., and D'Amico, S., 2004, Pool boiling heat transfer experiments in silica-water nano-fluids. *International Journal of Heat and Mass Transfer*, 47(2): 407-411.

[12] Zhou D. W., 2004, Heat transfer enhancement of copper nano.uid with acoustic cavitations. *Int. J. Heat Mass Transfer*; 47:3109–17.

[13] Gerardi, C., et al., 2011, Infrared thermometry study of nanofluid pool boiling phenomena, *Nanoscale Research Letters* 6:232-249.

[14] Bartolomei, G. G. and Chanturia, V. M. 1967, Experimental study of true void fraction when boiling subcooled water in vertical tubes, *Thermal Engineering*, 14, 123–128.

[15] Tolubinski, V.I., Kostanchuk, D.M., 1970, Vapor bubbles growth rate and heat

transfer intensity at subcooled water boiling, 4th Int. Heat Transfer Conf., Vol. 5, paper No. B-2.8, Paris.

[16] Kurul, M. Z., Podowski, 1990, Multidimensional effects in forced convection subcooled boiling, in: *Proceedings of the Ninth International Heat Transfer Conference*, August 19-24, Jerusalem, Israel, Vol. 2, pp. 21-26.

[17]Maiga, S. E. B. Nguyen, C. T., Galanis, N., and Roy, G. 2004, Heat Transfer Behaviors of Nanofluids in a Uniformly Heated Tube, *Journal of Superlattices and microstructures* 35, 543-557.

[18] Hamilton R. L., Crosser, O. K., 1962, Thermal Conductivity of Heterogeneous Two Component systems, *Industrial and Engineering Chemistry Fundamentals* 1/3, , 187-191.